Abnormal Reaction to Central Nervous System Injury in Mice Lacking Glial Fibrillary Acidic Protein and Vimentin

Milos Pekny,* Clas B. Johansson,[§‖] Camilla Eliasson,* Josefina Stakeberg,* Åsa Wallén,[¶] Thomas Perlmann,[¶] Urban Lendahl,[§] Christer Betsholtz,* Claes-Henric Berthold,[‡] and Jonas Frisén[§]

*Department of Medical Biochemistry and [‡]Department of Anatomy and Cell Biology, Gothenburg University, SE-405 30 Gothenburg, Sweden; and [§]Department of Cell and Molecular Biology, Medical Nobel Institute, [‖]Department of Neuroscience, Karolinska Institute and [¶]Ludwig Institute for Cancer Research, Stockholm Branch, SE-17177 Stockholm, Sweden

Abstract. In response to injury of the central nervous system, astrocytes become reactive and express high levels of the intermediate filament (IF) proteins glial fibrillary acidic protein (GFAP), vimentin, and nestin. We have shown that astrocytes in mice deficient for both GFAP and vimentin (GFAP−/−vim−/−) cannot form IFs even when nestin is expressed and are thus devoid of IFs in their reactive state. Here, we have studied the reaction to injury in the central nervous system in GFAP−/−, vimentin−/−, or GFAP−/−vim−/− mice. Glial scar formation appeared normal after spinal cord or brain lesions in GFAP−/− or vimentin−/− mice, but was impaired in GFAP−/−vim−/− mice that developed less dense scars frequently accompanied by bleeding. These results show that GFAP and vimentin are required for proper glial scar formation in the injured central nervous system and that some degree of functional overlap exists between these IF proteins.

Key words: GFAP • nestin • injury • astrocyte • blood vessel

A dense scar composed primarily of hypertrophic astrocytes forms rapidly at the site of a brain or spinal cord injury. Scar formation is thought to be important for recovering the tensile strength of the tissue and to shield intact parts of the central nervous system (CNS)[1] from secondary injury (Ridet et al., 1997). The astrocytic scar is very compact, which has led to the suggestion that it may act as a physical barrier to axonal growth. The role of scar formation in axonal regeneration has, however, been difficult to establish and remains controversial (reviewed in Frisén, 1997 and Ridet et al., 1997).

Various types of insults to the CNS, such as mechanical injury, lead to high level expression of the intermediate filament (IF) proteins glial fibrillary acidic protein (GFAP) and vimentin in astrocytes (Eddleston and Mucke, 1993). In response to injury, astrocytes also express a third IF protein, nestin (Lendahl et al., 1990; Clarke et al., 1994; Frisén et al., 1995; Lin et al., 1995). These changes in IF protein expression result in increased density of IFs within the cells.

IFs of immature astrocyte precursors and astrocytes have been shown to be composed of nestin and vimentin (Schnitzer et al., 1981; Bignami et al., 1982; Lendahl et al., 1990). As astrocytes mature, GFAP becomes expressed and vimentin expression decreases, in some astrocytes to undetectable levels (Bovolenta et al., 1984; Pixley and de Vellis, 1984). Many glial cells, such as astrocytes in the corpus callosum and hippocampus, tanycytes and Bergmann glia coexpress GFAP and vimentin in the adult animal (de Vitry et al., 1981; Lazarides, 1982).

IFs have been implicated in many cellular processes in different tissues. Mutations in keratin genes result in skin blistering diseases and desmin deficiency leads to reduced tensile strength in muscle cells (Li et al., 1997; Fuchs and Cleveland, 1998). These examples demonstrate a role for IFs in providing mechanical strength to certain types of cells. The role of IFs in astrocytes has been difficult to establish. Manipulation of GFAP expression levels in vitro by overexpression or by the application of antisense oligonucleotides has implicated GFAP in astrocyte process formation and in growth regulation (Weinstein et al., 1991; Rutka and Smith, 1993; Toda et al., 1994). However, mutant mice in which the *GFAP* (Gomi et al., 1995; Pekny et al., 1995; McCall et al., 1996) or *vimentin* (Colucci-Guyon et al., 1994) genes have been inactivated appear

The first three authors contributed equally to this study.

Address correspondence to Dr. Milos Pekny, Department of Medical Biochemistry, University of Gothenburg, Box 440, SE-405 30 Gothenburg, Sweden. Tel.: 46 31 7733269. Fax: 46 31 416108. E-mail: milos.pekny@medkem.gu.se

1. *Abbreviations used in this paper:* BrdU, bromodeoxyuridine; CNS, central nervous system; GFAP, glial fibrillary acidic protein; HE, hematoxylin and erythrosin/eosin; IF, intermediate filament; IR, immunoreactivity.

© The Rockefeller University Press, 0021-9525/99/05/503/12 $2.00

grossly normal. Detailed analyses of GFAP−/− mice have revealed signs of altered neuronal function (Shibuki et al., 1996; McCall et al., 1996) and some GFAP−/− mice show late-onset CNS dysmyelination and locally impaired blood-brain barrier function (Liedtke et al., 1996). We have studied the ability of cultured astrocytes to instruct vascular endothelial cells to develop blood-brain barrier properties in vitro and found that astrocytes from GFAP−/− mice failed to do so (Pekny et al., 1998a). Using primary cultures from GFAP−/− mice, we found that the ability of astrocytes to extend processes in response to contact with neurons was preserved, but proliferation was increased in such cultures (Pekny et al., 1998b).

Vimentin null mice have a reduced capacity to regulate vascular tone when challenged by ablation of renal tissue (Terzi et al., 1997). Furthermore, in the absence of vimentin, astrocyte IFs are composed solely of GFAP and form abnormally compact bundles (Eliasson, C., C.-H. Berthold, and M. Pekny, unpublished data). Scar formation after CNS injury appears normal in both GFAP−/− or vimentin−/− mice (Pekny et al., 1995; Galou et al., 1996). Similarly, GFAP−/− mice exhibit normal response to scrapie infection (Gomi et al., 1995; Tatzelt et al., 1996). However, it is likely that GFAP and vimentin in part have overlapping functions and that one protein may be able to compensate for the lack of the other protein in mutant mice.

We have generated mice carrying null mutations in both the *GFAP* and *vimentin* genes (GFAP−/−vim−/−) and observed that GFAP−/−vim−/− astrocytes lacked IFs completely in quiescent and reactive states in vivo as well as in vitro (Eliasson, C., C.-H. Berthold, and M. Pekny, unpublished data). GFAP−/−vim−/− mice can therefore be used to evaluate potential roles of IFs in astrocytic responses to injury. Here, we compared the reaction to mechanical brain or spinal cord injury in wild-type, GFAP−/−, vimentin−/−, or GFAP−/−vim−/− mice. We demonstrate that GFAP−/−vim−/− mice exhibit abnormal glial scar formation in response to injury in the CNS.

Materials and Methods

Animals

Mice with null mutations in the *GFAP* (Pekny et al., 1995) or *vimentin* (Colucci-Guyon et al., 1994) genes were crossed to generate double mutants. These mice reached adulthood and did not display any overt anatomical or behavioral defects. Genotypes were determined as described (Colucci-Guyon et al., 1994; Pekny et al., 1995). All the mice used in these studies were on C57BL/129 mixed genetic background and were maintained in a conventional animal facility.

Spinal Cord and Brain Injuries

Mice subjected to spinal cord or brain injury were killed shortly after the injury (2 or 3 d) or were allowed to survive for 2 or 3 wk. In one group of animals the spinal cord dorsal funiculus was transected at the upper thoracic level, and the injury was extended 5 mm rostrally by a longitudinal incision (Frisén et al., 1992). In other animals, a 27-G needle was inserted through the skull and into the frontal cerebral cortex. After both types of injury, wild-type, GFAP−/−, or vimentin−/− animals did not display any recognizable symptoms after any of the lesions. The following number of animals were used for the spinal cord injury studies (shown as number of animals allowed to survive 2 d, 2 wk): wild-type (n = 10, 5), GFAP−/− (n = 8, 4), vimentin−/− (n = 2, 2), and GFAP−/−vim−/− (n = 3, 3). For the brain injury, these animals were used (shown as number of animals allowed to survive 3 d, 3 wk): wild-type (n = 3, 3), GFAP−/− (n = 4, 3), vimentin−/− (n = 2, 2), and GFAP−/−vim−/− (n = 5, 3).

Nestin Immunohistochexmistry

Tissues were fixed by transcardial perfusion of anesthetized mice with Tyrode's solution followed by 4% formaldehyde and 0.4% picric acid in PBS or immersion fixation in Bouin's fixative (75 ml of saturated picric acid, 5 ml of glacial acetic acid, 25 ml of 40% formaldehyde). Specimens were cryosectioned or embedded in paraffin and sectioned using a microtome. Sections from all animals were stained with hematoxylin and erythrosin/eosin (HE) using standard protocols. Immunohistochemistry with rabbit antiserum to nestin (no. 130, diluted 1:2,000; Dahlstrand et al., 1992; Tohyama et al., 1992) was performed as described (Frisén et al., 1995; Pekny et al., 1998b). Binding of primary antibodies was visualized with Cy2-conjugated donkey anti–rabbit antibodies (Jackson ImmunoResearch) or HRP-conjugated goat antiserum against rabbit immunoglobulins (Dako A/S). Peroxidase was detected with DAB (Dako A/S). Photomicrographs were scanned and mounted using Adobe Photoshop.

In Situ Hybridization

Nestin mRNA expression in the injured spinal cord was detected by in situ hybridization using digoxigenin labeled cRNA probes as described by Schaeren-Wiemers and Gerfin-Moser (1993). The animals were allowed to survive 4 d after the incision in the dorsal funiculus. The antisense probe was prepared with T3 RNA polymerase from a NotI linearized plasmid containing a mouse nestin cDNA corresponding to nucleotides 1630–2972 (according to GenBank accession number M34384) and the sense probe was generated with T7 polymerase from the same plasmid linearized with XhoI. No specific hybridization was seen with the sense probe.

Detection of Bromodeoxyuridine and S-100

Two mice of each genotype were used for the bromodeoxyuridine (BrdU) incorporation experiments. 1 h after the brain injury, which was performed as described above, the mice were injected i.p. with BrdU (100 μg/g body weight). The injections were repeated 17 times for 50 h; injections were applied every second hour with a 10-h injection-free window each night. The mice were anesthetized and transcardially perfused with 0.1 M phosphate buffer followed by 4% paraformaldehyde. Vibratome or frozen sections were used for either simultaneous or sequential detection of BrdU and S-100. For BrdU detection sections were treated with 2 M HCl for 30 min followed by 0.25% pepsin in 0.1 M HCl for 2 min at 37°C before incubation with the primary antibody. Mouse monoclonal antibody (M0744) and goat anti–mouse FITC-conjugated antibody (F0479; both Dako A/S) were used. For S-100 immunodetection, rabbit anti–cow S-100 antibody (Z311) was used followed by swine anti-rabbit TRITC-conjugated antibody (R0156; both Dako A/S).

Electron Microscopy

The following genotypes and number of mice were used for ultrastructural analysis: wild-type (n = 4), GFAP−/− (n = 3), vimentin−/− (n = 2), and GFAP−/−vim−/− (n = 3). 3 d after a cortical stab wound, the mice were anesthetized and transcardially perfused with Tyrode's solution followed by 500 ml of a solution containing 2% paraformaldehyde and 2% glutaraldehyde dissolved in PBS. After postfixation overnight, the tissues were cut on an Oxford Vibratome and osmicated for 4 h, dehydrated in acetone, and embedded in Vestopal W. Ultra-thin sections (80–100 nm thick) were cut from injured brain cortex of all animals using an LKB Ultrotome. These sections measured 1.5 × 0.4 mm and included at one side the wound, covered the reaction zone, and displayed compact neuropile at the opposite side. The sections were picked up on Formvar-coated one-slot copper grids, contrasted with lead citrate (Reynolds, 1963) and uranyl acetate, and examined in a Philips EM 400 electron microscope.

Morphological Measurements

Blood vessel diameters were measured in cross sections of thoracic spinal cord segments in a microscope fitted with a scale in the eyepiece. The smallest distance across an individual blood vessels was assigned as the diameter of the blood vessel. The distance from the dorsal spinal cord surface to the bottom of the indentation in the dorsal funiculus was considered as the depth of the indentation below the superficial dorsal vessel

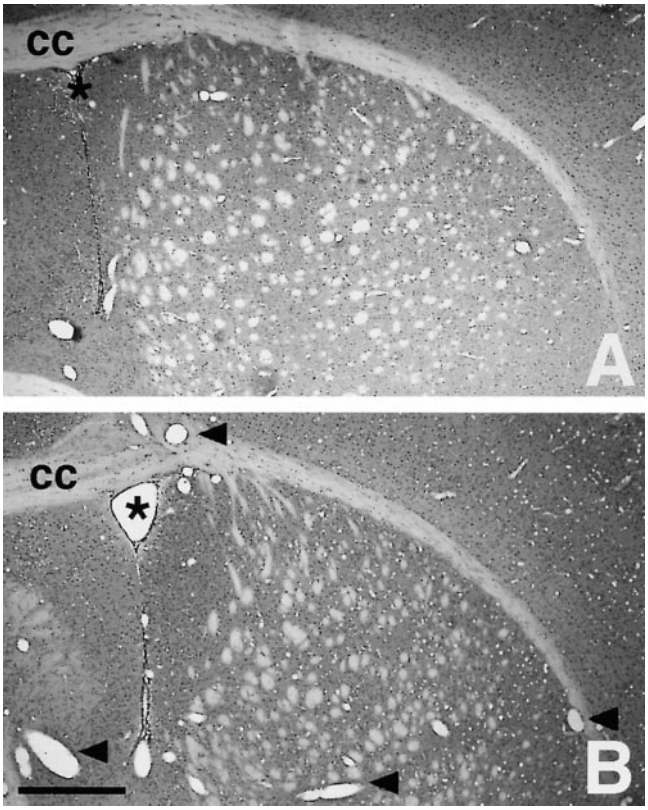

Figure 1. Blood vessel dilation. Hematoxylin and eosin stained coronal brain sections from wild-type (A) and GFAP−/−vim−/− (B) mice show an increased number of large diameter blood vessels in GFAP−/−vim−/− mice (some are indicated by arrowheads in B). The lumen of the lateral ventricle is indicated with an asterisk and the corpus callosum is labeled cc. Bar, 500 μm.

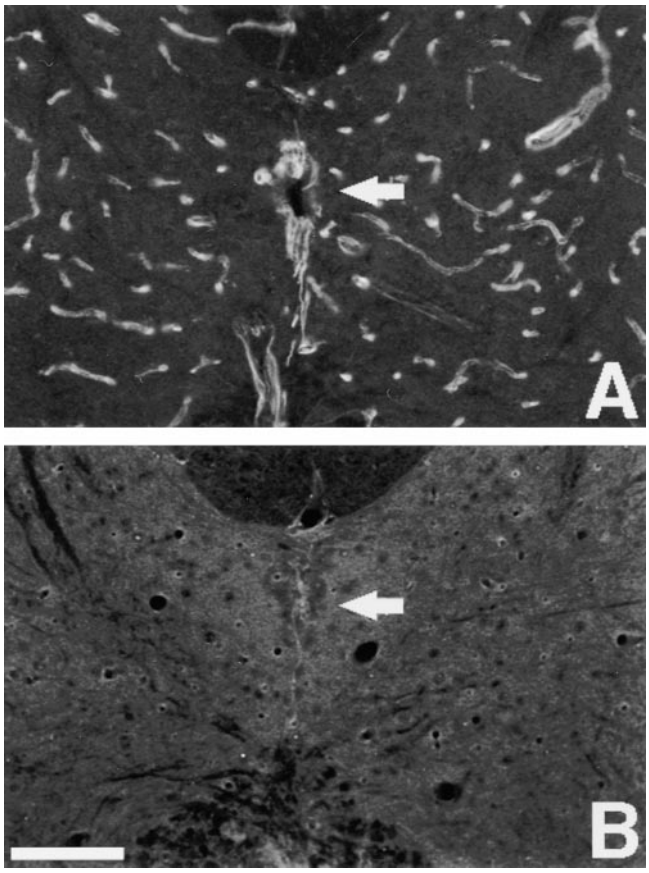

Figure 3. Altered nestin-IR in the absence of vimentin. Immunofluorescence localization of nestin in the uninjured spinal cord. (A) In a wild-type mouse, strong nestin-IR is seen in ependymal cells and endothelial cells. (B) Nestin-IR is weak and diffuse in vimentin−/− mouse. The arrows indicate the localization of the central canal. Bar, 100 μm.

(dorsal spinal vein). The genotypes of the animals were unknown to the person performing the measurements. Blood vessel diameters and dorsal funiculus indentations were measured in at least six animals of each genotype and at least 4 sections were analyzed from each animal. The average number of blood vessels wider than 15 μm per section and the average depth of the indentation in the dorsal spinal cord was calculated for each animal, and were used to calculate the mean and standard error of the mean for animals of each genotype. Statistical significance was tested by Student's two-tailed *t* test. The differences were considered significant if the *P* values were lower than 0.01.

Results

Dilated Blood Vessels and Altered Nestin Expression in Endothelial and Ependymal Cells

We first analyzed the uninjured nervous system of the mutant mice. Many blood vessels appeared dilated in the brain and spinal cord of GFAP−/−vim−/− mice (Fig. 1). The lumina of these structures were lined with von Willebrand factor–immunoreactive endothelial cells indicating that they were true blood vessels rather than, for example, cavities formed by degeneration (data not shown). Measurements of blood vessel diameters in these mice revealed an almost threefold increase in the number of blood vessels with a diameter >15 μm compared to wild-type mice ($P < 0.0005$; Fig. 2 A). We frequently noticed that there was an unusually deep indentation in the tissue

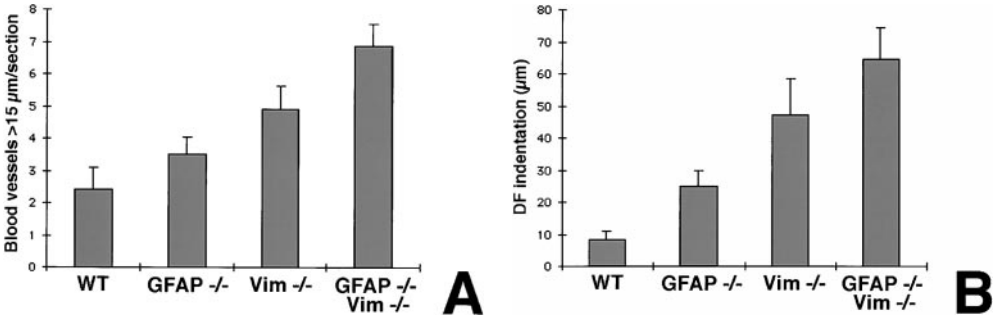

Figure 2. Quantification of blood vessel dilation and the indentation below the dorsal spinal vein. (A) Average number of blood vessels with a diameter greater than 15 μm in spinal cord sections of mice of different genotypes. (B) Depth of the indentation in the spinal cord dorsal funiculus. Bars indicate SEM.

of the dorsal spinal cord in many of the mutant mice. In wild-type mice, there is often an invagination below the dorsal spinal vein, but measurements of the depth of the invagination revealed a statistically significant increase in the depth compared to wild-type mice in GFAP−/− ($P < 0.005$), vimentin−/− ($P < 0.0001$), and GFAP−/−vim−/− mice ($P < 0.0001$; Figs. 2 B and 6, A–D).

Endothelial and ependymal cells in the adult CNS express both nestin (Dahlstrand et al., 1992; Frisén et al., 1995; Fig. 3 A) and vimentin (Franke et al., 1979), but not GFAP in wild-type mice. Nestin-immunoreactivity (IR) in these cells appeared normal in GFAP−/− mice (data not shown). However, in vimentin−/− mice, nestin-IR was reduced to very low levels in both endothelial and ependymal cells (Fig. 3 B). Moreover, nestin-IR did not display a filamentous pattern but was spread diffusely throughout the cytoplasm in these cells (Fig. 3 B). The same nestin-IR pattern was seen in GFAP−/−vim−/− mice (data not shown).

Defective Glial Scar Formation after Spinal Cord Injury in GFAP−/−vim−/− Mice

We next analyzed scar formation in wild-type and mutant mice in response to an incision in the spinal cord dorsal funiculus. The mice were allowed to survive 2 d or 2 wk after the injury, and tissue sections from the site of the injury and from a spinal cord segment 10 mm rostral to the lesion were analyzed. There were no consistent differences in the histology of the scar tissue between wild-type, GFAP−/−, or vimentin−/− mice revealed by HE staining (Fig. 4). However, the scar tissue was much less dense in the GFAP−/−vim−/− mice, and the scar tissue was interrupted by numerous fissures most often running in a dorso-ventral orientation (Fig. 4, H and L). These fissures were filled with blood, tissue fluid or debris (Fig. 4 L). Moreover, in the GFAP−/−vim−/− animals there was a large number of red blood cells within the scar tissue, both 2 d and 2 wk after the injury, indicating more pronounced bleeding and/or defective clearance of blood from the injury site (Fig. 4, H and L).

Nestin Expression in the Injured Spinal Cord

Nestin expression is rapidly induced in astrocytes after CNS injury and serves as a sensitive marker for reactive astrocytes (Clarke et al., 1994; Frisén et al., 1995; Lin et al., 1995). Nestin-IR was induced in response to spinal cord injury in mice of all genotypes (Fig. 5). However, nestin-IR was more restricted in vimentin−/− or GFAP−/−vim−/− mice compared to wild-type or GFAP−/− mice (Fig. 5). Whereas 2 d after the injury nestin-IR cells were seen at the site of the lesion and in the surrounding gray matter in wild-type (Frisén et al., 1995) or GFAP−/− mice, nestin-IR was less pronounced in the gray matter in vimentin−/− or GFAP−/−vim−/− mice (Fig. 5). Furthermore, 2 wk after the lesion the levels of nestin-IR in the scar were lower in vimentin−/− or GFAP−/−vim−/− mice compared to wild-type or GFAP−/− mice (Fig. 5). Whereas the scar tissue appeared dense after 2 wk in wild-type, GFAP−/− or vimentin−/− mice, the labeled cells were more sparse in GFAP−/−vim−/− mice and nestin-IR was diffusely spread throughout the cytoplasm of the cells (Fig. 5). Nestin-IR was induced within 2 d after the injury in segments rostral to the lesion, in the degenerating axonal tract, to a similar extent in mice of all genotypes (Fig. 6). However, 2 wk after the injury the level of nestin-IR in the degenerating tract had decreased substantially in the

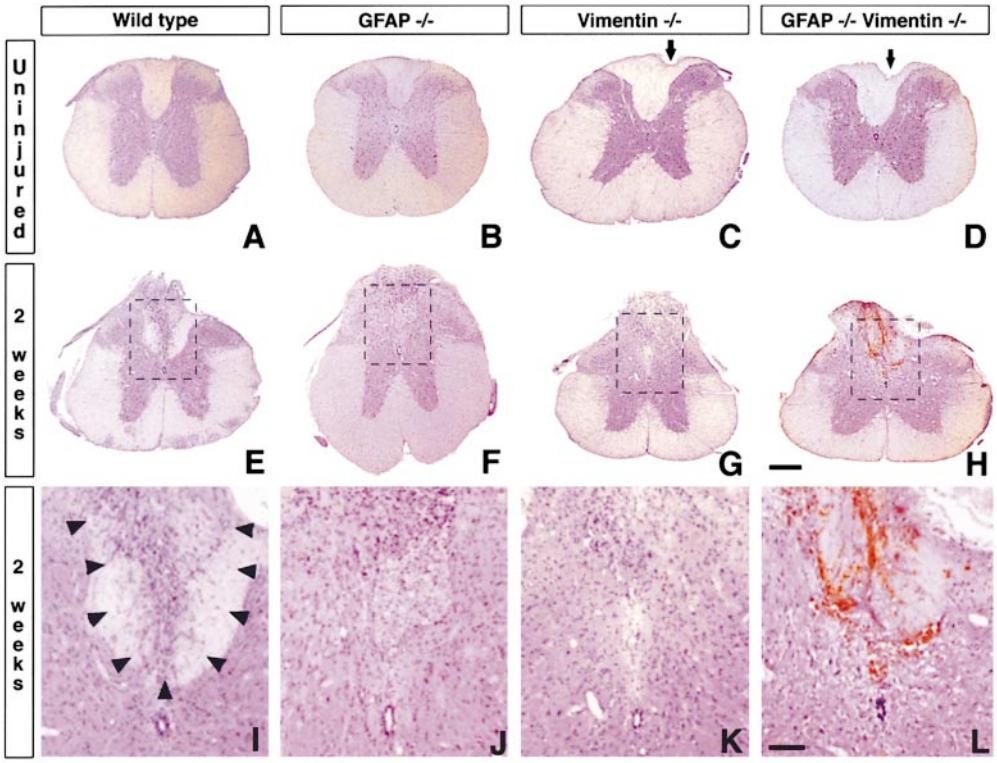

Figure 4. Structure of the uninjured and injured spinal cord in wild-type and mutant mice. The micrographs show hematoxylin and eosin stained transverse sections of upper thoracic spinal cord from uninjured animals and from animals in which the dorsal funiculus was transected 2 wk before analysis. The arrows in C and D indicate invaginations in the dorsal funiculus. In I–L, details indicated by hatched boxes in E–H are shown at higher magnification. The injured area is demarcated by arrowheads in I. Note the abundance of erythrocytes at the injury in H and L. Bars: (H) 300 μm; (L) 100 μm.

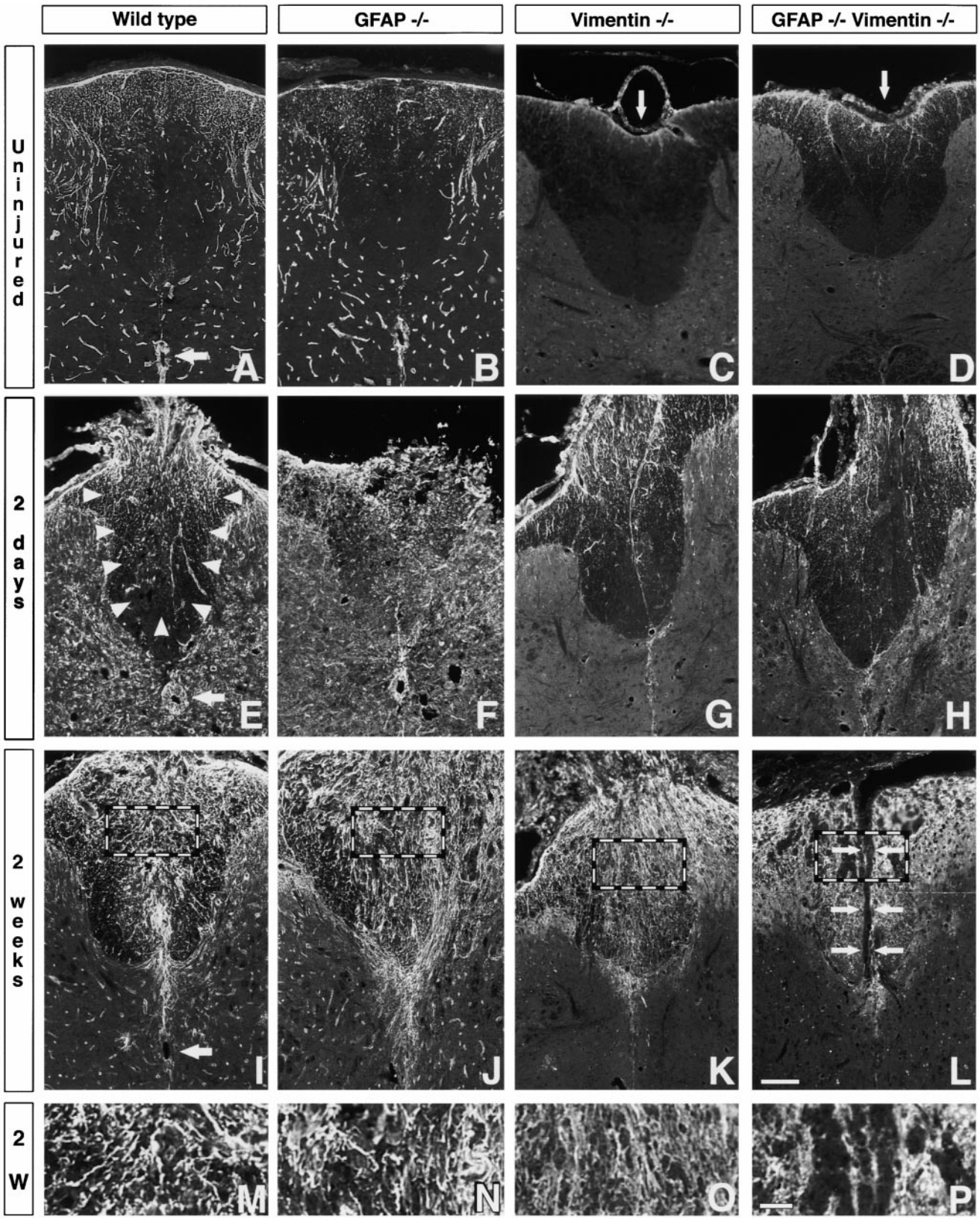

Figure 5. Nestin-IR at a spinal cord lesion in wild-type and mutant mice. Nestin-IR in the uninjured spinal cord and 2 d or 2 wk after a dorsal funiculus incision. Nestin-IR is induced at the injury in mice of all genotypes, but is weaker and more diffuse in vimentin −/− and GFAP−/−vim−/− mice compared with wild-type and GFAP−/− mice in E–P. The location of the central canal is indicated by arrows in A, E, and I. The arrow in D points at an indentation in the dorsal funiculus. The arrowheads in E indicate the approximate area affected by the injury. The arrows in L mark a fissure in the dorsal funiculus. The areas indicated by hatched boxes in I–L are shown at higher magnification in M–P. Bars: (L) 100 μm; (P) 30 μm.

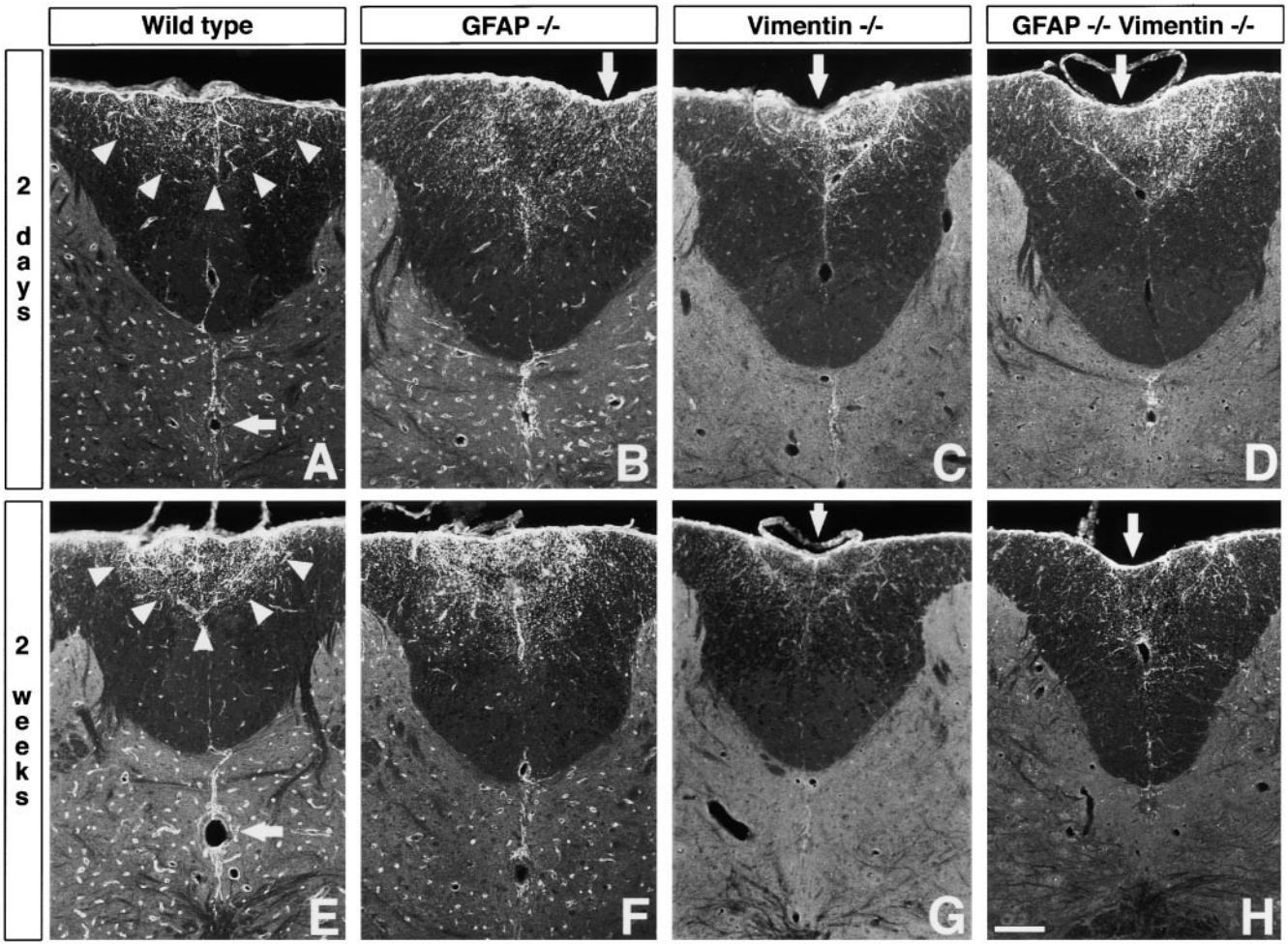

Figure 6. Nestin-IR in degenerating axonal tracts in wild-type and mutant mice. Nestin-IR in sections taken 10 mm rostral to a dorsal funiculus incision 2 d or 2 wk after the injury. Nestin-IR is induced in astrocytes in the dorsal and central part of the dorsal funiculus (indicated by arrowheads in A and E) due to Wallerian degeneration. The induction of nestin-IR is more transient in vimentin −/− or GFAP−/−vim−/− mice compared with wild-type or GFAP−/− mice. The arrows in A and E indicate the location of the central canal and the arrows in B–D, G, and H point at invaginations in the dorsal funiculus. The dorsal spinal vein located in the invagination is often destroyed during tissue processing but can be seen in D and G. A few wide blood vessels are indicated by arrowheads in G. Bar, 100 μm.

vimentin−/− or GFAP−/−vim−/− mice, whereas it remained strong in wild-type or GFAP−/− mice (Fig. 6).

To determine whether the reduced nestin-IR in the injured spinal cord was caused by reduced transcription of the *nestin* gene in vimentin−/− and GFAP−/−vim−/− mice, we performed in situ hybridization with *nestin* antisense riboprobes in spinal cord sections from animals that underwent a dorsal funiculus incision 4 d before. *Nestin* mRNA was detected in mice of all genotypes, and no reduction in *nestin* mRNA levels could be found in vimentin−/− and GFAP−/−vim−/− mice (Fig. 7). Scattered cells in the dorsal funiculus expressed nestin mRNA and their distribution was highly reminiscent of the nestin-IR pattern. No specific hybridization was seen with the sense probe (Fig. 7, E and F).

Responses to Brain Injury

Glial scar formation was also analyzed in the brain. A cortical stab wound was done with a fine needle, resulting in a much more restricted injury than the spinal cord lesion. Interestingly, 3 out of 11 GFAP−/−vim−/− mice died shortly after the injury and the necropsy showed extensive intracranial bleeding that was interpreted as the cause of death (data not shown). In the group of GFAP−/−vim−/− mice that were killed 3 d after the injury, 3 out of 5 mice showed extensive bleeding at the site of injury (Fig. 8 D). Bleeding of comparable magnitude was not seen in mice of other genotypes. In all wild-type, GFAP−/− and vimentin−/− mice, as well as in the GFAP−/−vim−/− mice that survived the operation, the discrete injury caused by the needle did not cause any apparent clinical symptoms and was sealed within 3 wk (Fig. 8). Nestin-IR was detected around the cortical lesion 3 d after the injury in mice of all genotypes (Fig. 8). However, whereas nestin-IR was comparably strong and revealed distinct reactive astrocytes in both wild-type and GFAP−/− mice, it was weaker and diffuse in vimentin−/− and GFAP−/−vim−/−

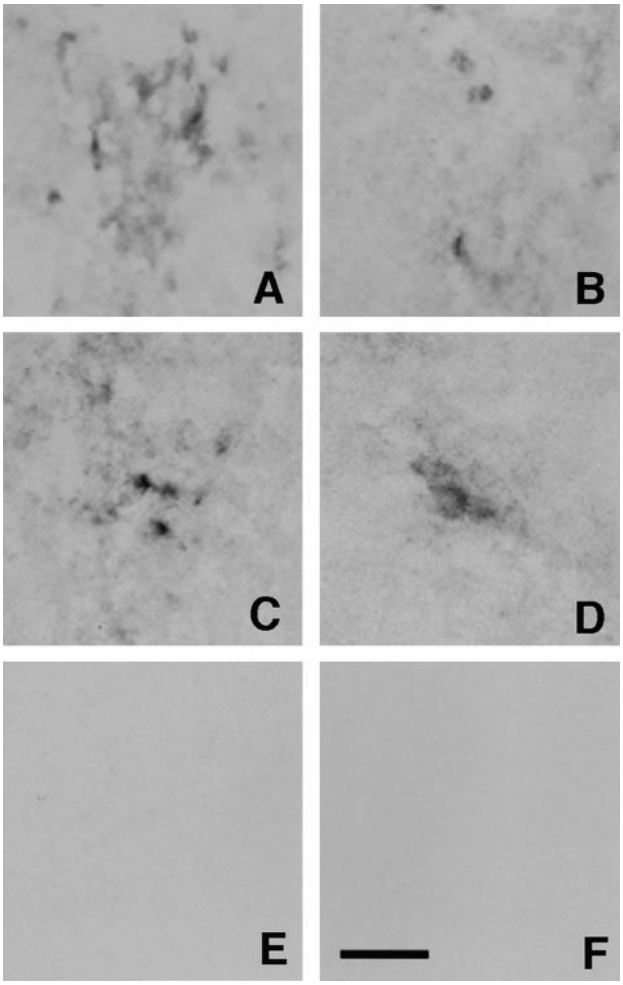

Figure 7. Nestin mRNA expression in the injured spinal cord. A digoxigenin labeled riboprobe was used to localize nestin mRNA in the spinal cord 4 d after an incision in the dorsal funiculus. Nestin mRNA is expressed in scattered cells at the injury site in wild-type (A), GFAP−/− (B), vimentin−/− (C), and GFAP−/−vim−/− mice (D). The micrographs show details from the dorsal funiculus. No specific hybridization was seen with sense probes in adjacent sections from wild-type (E) or GFAP−/−vim−/− (F) mice. Bar, 50 μm.

mice (Fig. 8, G and H). Nestin-IR was reduced to undetectable levels after 3 wk in mice of all genotypes (data not shown).

Ultrastructural Analysis of Scar Formation

To further characterize scar formation in the mutant mice, we analyzed the zone immediately adjacent to the central necrotic area of cortical injury by electron microscopy. This area was similar in wild-type, GFAP−/−, or vimentin−/− mice, but differed in GFAP−/−vim−/− mice. The difference was most apparent in the border zone between the severely disarranged tissue close to the wound and the more distant, compact and normal looking brain tissue. Here, the GFAP−/−vim−/− mice exhibited fragmented tissue with a high accumulation of extracellular debris. This debris was diffuse, finely granular or filamentous of moderate electron density (Fig. 9 d). This was in contrast to mice of the other genotypes (Fig. 9, a–c) in which the brain tissue in the corresponding area showed easily identifiable components (e.g., myelinated and unmyelinated axons, synaptosome-like profiles), narrow extracellular spaces and virtually no extracellular debris.

Cell Proliferation after the Cortical Injury

To evaluate cell proliferation in the area affected by the cortical injury we have compared BrdU incorporation within a 50-h time window after the injury in wild-type, GFAP−/−, vimentin−/−, and GFAP−/−vim−/− mice. Using confocal microscopy we have counted BrdU-labeled cells within the volume of 5×10^6 μm^3 that included the injury area in the middle and was reconstructed from superimposed confocal images. The number of BrdU-labeled cells within this volume ranged from 64 to 87 and no statistically significant differences were found between wild-type and mutant mice. To determine the proportion of astrocytes among the BrdU-labeled cells, S-100 positive cells were counted within the same volume. The number of S-100 positive cells ranged from 65 to 83 and no statistically significant differences were found between wild-type and mutant mice. Fig. 10 provides a comparison between individual (Fig. 10, a–d) and combined (Fig. 10, e and f) BrdU and S-100 immunostaining of the cortical injury area in wild-type and GFAP−/−vim−/− mice. Both contain comparable numbers of BrdU positive, S-100 positive and double positive cells (some of these are indicated by arrows). Thus, the cortical injury in wild-type and mice deficient for GFAP and/or vimentin triggers a comparable induction of cell division.

Discussion

The role of astrocytic IF proteins has been the subject of numerous studies, but has been difficult to establish. In this study we have utilized mice carrying null mutations in the *GFAP* and/or *vimentin* genes. We found that GFAP and vimentin have partly overlapping functions in the astrocytic response to injury, and contribute to scar formation. Furthermore, blood vessel dilation was seen in the brain and spinal cord of mice lacking both vimentin and GFAP.

Altered Nestin Expression in Endothelial and Ependymal Cells and Dilation of Blood Vessels

In the nervous system of adult wild-type mice, nestin expression is largely restricted to endothelial and ependymal cells (Dahlstrand et al., 1992; Frisén et al., 1995). Both of these cell types also express vimentin (Franke et al., 1979; Schnitzer et al., 1981). The nestin expression pattern was distinctly altered in vimentin−/− or GFAP−/−vim−/− mice. In wild-type or GFAP−/− mice, nestin-IR in endothelial or ependymal cells exhibited a distinct pattern in contrast to the weak and diffuse nestin-IR seen in vimentin−/− or GFAP−/−vim−/− mice (Fig. 3 and data not shown). Analysis of reactive astrocytes in vivo and astrocytes in culture from GFAP−/−vim−/− mice revealed the lack of IFs in these cells in spite of nestin expression, demonstrating that nestin fails to form IFs on its own in astrocytes (Eliasson et al., unpublished observations). The in

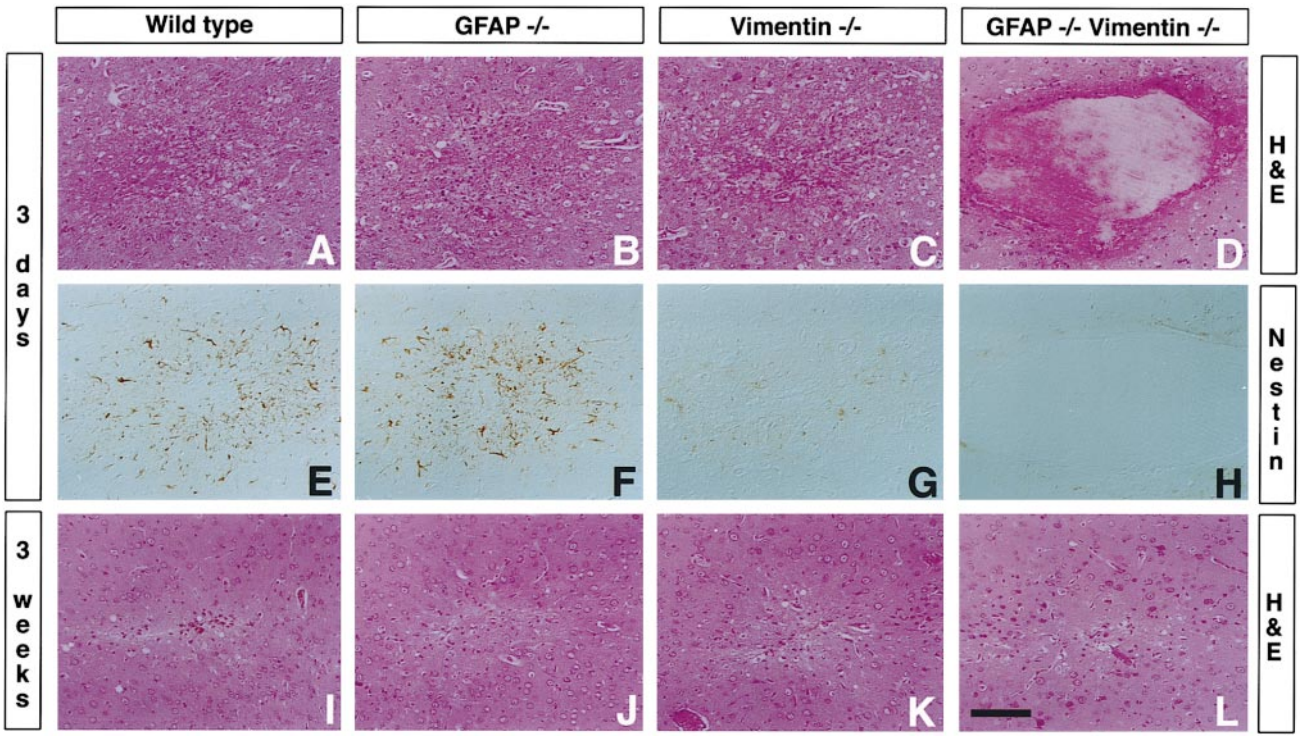

Figure 8. Response to cortical injury in wild-type and mutant mice. Hematoxylin and erythrosin staining and nestin-IR in adjacent sections of frontal cortex from mice 3 d or 3 wk after a fine needle cortical injury. In most of GFAP−/−vim−/− mice 3 d after the injury, bleeding was detected within the lesion zone (D). Nestin-immunoreactive cells can be seen in the lesion area in all animals 3 d after the injury, but the labeling appears weaker and more diffuse in the cells of vimentin−/− and GFAP−/−vim−/− mice (G and H). The injury was sealed in animals of all genotypes 3 wk after this type of injury (I–L). Bar, 100 μm.

situ hybridization data did not reveal any reduction in nestin mRNA expression in the spinal cord of vimentin−/− or GFAP−/−vim−/− mice compared to wild-type. This implies that the differences detected at the level of nestin-IR are posttranslational, probably caused by the changed equilibrium between unpolymerized and polymerized nestin in a situation when nestin polymerization cannot occur. This is further supported by the results from the Northern blot analysis of the RNA from astrocytes in vitro that showed rather an increase in nestin transcription in vimentin−/− and GFAP−/−vim−/− astrocytes (Eliasson et al., unpublished observations). Two-hybrid analysis has further indicated that nestin cannot bind to itself and nestin also fails to form IFs in SW13 cells devoid of other IF proteins, but incorporates into IFs once vimentin or desmin is transfected into these cells (Sjöberg, G., and T. Sejersen, personal communication; Marvin et al., 1998). These data suggest that the altered nestin-IR pattern observed in endothelial and ependymal cells in vimentin−/− or GFAP−/−vim−/− mice reflects the failure of nestin to form IFs in the absence of other IF proteins also in these cells.

Many blood vessels were dilated in the brain and spinal cord in GFAP−/−vim−/− mice. Vimentin, but not GFAP, is normally expressed both in endothelial cells and in perivascular cells such as pericytes and smooth muscle cells (Franke et al., 1979; Gabbiani et al., 1981). A reduction or lack of IFs in endothelial and perivascular cells may decrease the mechanical strength of blood vessels and consequently their capacity to withstand dilation. The observed increase in blood vessel diameter in the CNS of GFAP−/−vim−/− mice may be caused by altered properties of endothelial or perivascular cells (as a consequence of vimentin absence in these cells) and a reduced capacity of the surrounding tissue to withstand blood vessel dilation (the consequence of absence of GFAP and vimentin in astroglial cells). Such a concept is supported by the finding of a progressively deeper indentation beneath the dorsal spinal vein in GFAP−/−, vimentin−/−, and in GFAP−/−vim−/− mice, respectively.

Defective CNS Scar Formation in GFAP−/−vim−/− Mice

Scar formation after a spinal cord or brain injury appeared comparable in wild-type, GFAP−/−, or vimentin−/− mice, but was defective in mice lacking both GFAP and vimentin, indicating that these proteins may have partly overlapping functions in this process. In such mice, the glial scar was less compact, contained more debris compared to the mice of the other genotypes, and the scar tissue was disrupted by fissures. Using BrdU incorporation, we did not detect any differences in cell proliferation in the injury area. Also, the amount of astrocytes, detected as S-100 positive cells, in the injury area was comparable between the mice of different genotypes. These results imply

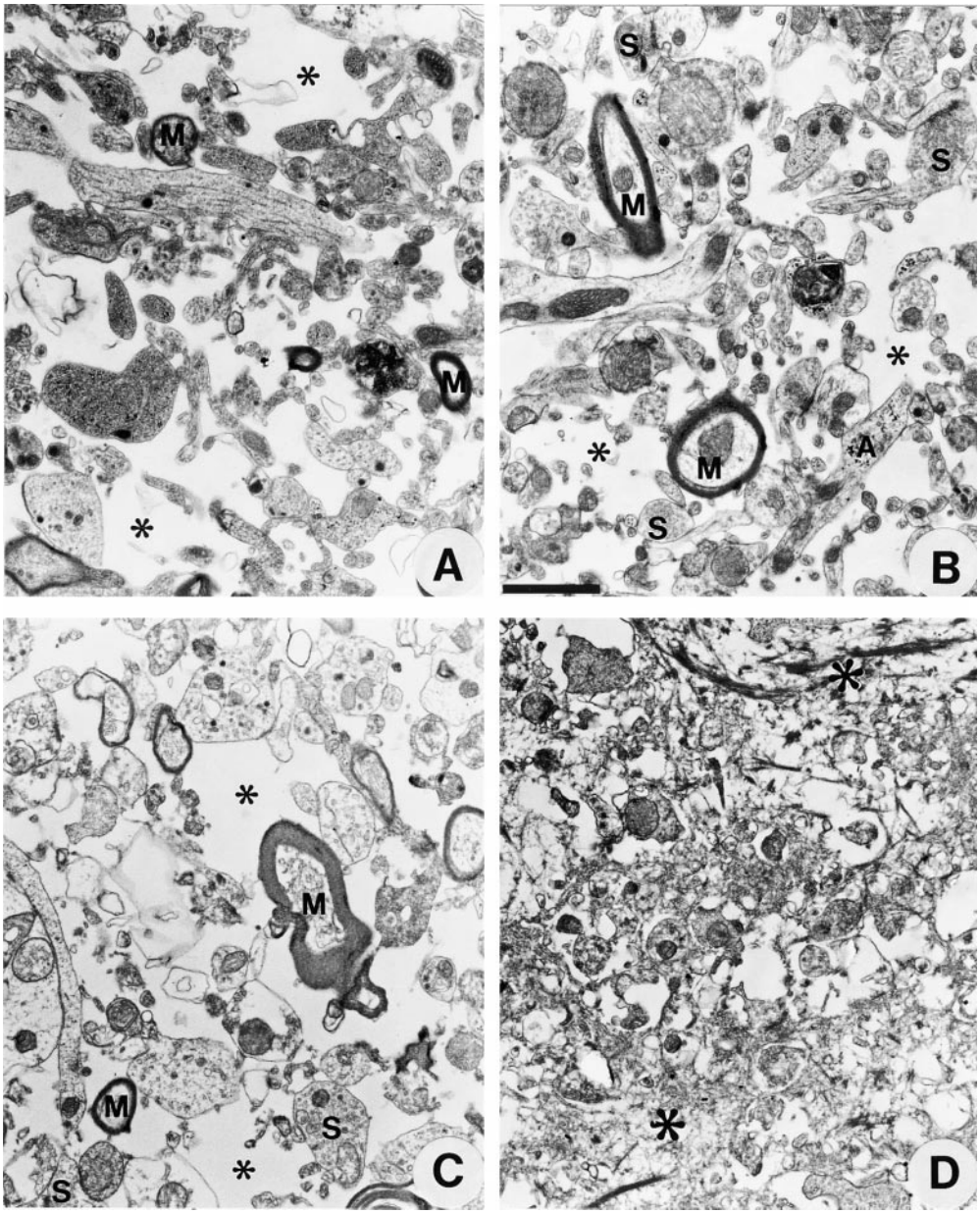

Figure 9. Ultrastructural analysis of a cortical stab wound. Electron micrographs of the frontal cerebral cortex 3 d after the injury. The pictures show the border zone between the spongy tissue of the wounded area and the surrounding compact cortical tissue. In wild-type (A), GFAP−/− (B), or vimentin−/− (C) mice, the extracellular space (small asterisk) is restricted and free of debris. In GFAP−/− vim−/− mice the extracellular space is filled with masses of filamentous and diffuse debris (large asterisk). A, astrocytic profile; M, myelinated axon; S, synaptosome-like profile. Bar, 1 μm.

that even in GFAP−/−vim−/− mice, the injury results in a normal response at the level of cell proliferation.

Major similarities exist between the epithelial response to injury and reactive gliosis in the CNS. In both cases, production of IF proteins accompanies cell activation and the process results in the closure of the wound. In case of stratified epithelia, such as the epidermis of the skin, the wound closure happens in an orchestrated action of keratinocyte migration from the surrounding healthy tissue and a contraction of the connective wound bed mediated by migrating fibroblasts (for review see McGowan and Coulombe, 1998). Keratinocyte activation and migration parallel induction of the wound repair-associated IF proteins in these cells, namely keratins 6, 16, and 17, which happens within 6–12 h after injury (Paladini et al., 1996). In the injured CNS, proliferation of stem cells is induced by injury, and the progeny of the stem cells migrate towards the injury where they differentiate to astrocytes (Johansson et al., 1999). Thus, cell migration and wound contraction may be phenomena playing a major role in wound closure in general. Our preliminary experiments suggest that in the scrape wounding assay in vitro, cultures of GFAP−/−vim−/− astrocytes require longer time to close the defect (unpublished data). Therefore, it is possible that reactive astrocytes without IFs exhibit a cell migration deficit. To address the contractile properties of astrocytes from wild-type and GFAP and/or vimentin deficient mice, we investigated whether primary cultured astrocytes from these mice can contract collagen gels. All type of astrocytes were able to contract the gels and no quantitative differences between wild-type, GFAP−/−, vimentin−/−, and GFAP−/−vim−/− astrocytes were detected (data not shown).

The defective scar formation in GFAP−/−vim−/−

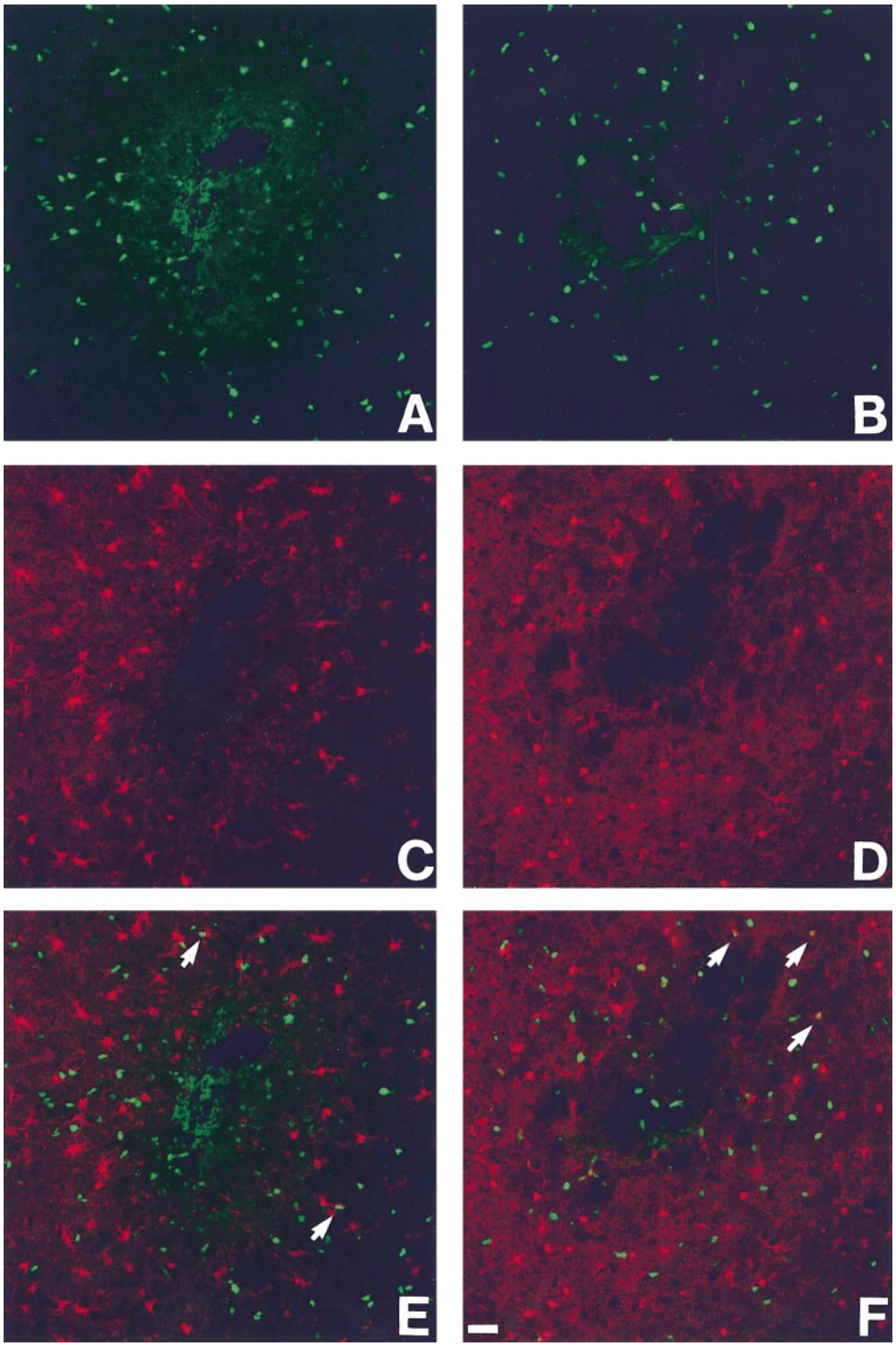

Figure 10. Cell proliferation in the injury area in wild-type and mutant mice. Confocal images of BrdU labeling (A and B) and S-100 IR (C and D) in the area of brain cortical injury. No difference is apparent between wild-type and GFAP−/−vim−/− mice. Combined labeling reveals a proportion of double positive cells (E and F; some of them indicated by an arrow). Confocal pictures are maximal projections of superimposed images covering the thickness of 12 μm. Bar, 50 μm.

mice may not only be a result of astrocytic dysfunction but may also relate to the abnormal blood vessels seen in these mice. It is unlikely that the blood vessel abnormality is the major reason for defective scar formation in these mice, since scar formation appeared normal in vimentin−/− mice and only vimentin, and not GFAP, is expressed in cells of the blood vessel. The bleeding seen in GFAP−/−vim−/− mice therefore probably results from the combination of abnormal blood vessels and defective closure of the wound.

The amount of debris was clearly elevated in glial scar tissue of GFAP−/−vim−/− mice compared to mice of the other genotypes. This can either be a result of defective clearance of tissue debris or its increased production. Astrocytes are capable of phagocytosis and the abundance of debris in GFAP−/−vim−/− mice may result from im-

pairment of this function. Alternatively, the bleeding observed in GFAP−/−vim−/− mice may result in the formation of more debris in the forming glial scar and its immediate vicinity.

Multiple fissures traversed through the scar in the injured spinal cord of GFAP−/−vim−/− mice. This may be a consequence of reduced astrocytic process formation with deficient bridging and sealing of the wound. Absence of IFs in astrocytes is likely to reduce the tensile strength of individual astrocytes, and as a consequence, of the tissue. A low resistance to mechanical forces is likely to inhibit scar formation, especially in the spinal cord that has to adapt to movements of the vertebral column, a situation distinct from that in the skull-enclosed brain. Irrespective of its cause, defective scar formation may lead to repeated tearing of the tissue and recurring bleeding, potentially explaining the abundance of red blood cells in the scar tissue of GFAP−/−vim−/− mice. The defective glial scar formation in GFAP−/−vim−/− mice described here reveals the importance of GFAP and vimentin for this process as well as a certain degree of functional overlap between these two proteins.

We wish to thank Dr. Kristofer Rubin for performing the collagen gel contraction assays, Dr. Charles Babinet for providing the vimentin null mice, Dr. Martha Marvin for the gift of nestin cDNA, Dr. Charles Babinet and Dr. Alain Privat for valuable discussions, Ms. Ulrika Wilhemsson for genotyping some of the animals, and Ms. Marianne Eriksson and Ms. Rita Grandér for technical help with processing the tissue for electron microscopy.

This study was supported by grants from the Swedish Medical Research Council (project nos. 11548, 09041, 12183, and 03157), the Swedish Cancer Foundation (project no. 3622), the King Gustav V Foundation, the Swedish Society for Medicine, the Swedish Society for Medical Research, A$^+$ Science Invest, Stiftelsen Sigurd och Elsa Goljes minne, Stiftelsen Lars Hiertas Minne, Björklunds fond, Jeanssons stiftelse, Ostermans stiftelse, Magnus Bergvalls stiftelse, Marcus Borgströms stiftelse, Tore Nilssons stiftelse, the Wenner-Gren foundations, Åke Wibergs stiftelse, Kapten Arthur Erikssons fond, Inga-Britt and Arne Lundberg foundation, and Gustafsson foundation. M. Pekny was supported by a fellowship from the Swedish Society for Medical Research.

Received for publication 17 April 1998 and in revised form 17 March 1999.

References

Bignami, A., T. Raju, and D. Dahl. 1982. Localization of vimentin, the nonspecific intermediate filament protein, in embryonal glia and in early differentiating neurons. In vivo and in vitro immunofluorescence study of the rat embryo with vimentin and neurofilament antisera. *Dev. Biol.* 91:286–295.

Bovolenta, P., R.K. Liem, and C.A. Mason. 1984. Development of cerebellar astroglia: transition in form and cytoskeletal content. *Dev. Biol.* 102:248–259.

Clarke, S.R., A.K. Shetty, J.L. Bradley, and D.A. Turner. 1994. Reactive astrocytes express the embryonic intermediate neurofilament nestin. *Neuroreport.* 5:1885–1888.

Colucci-Guyon, E., M.M. Portier, I. Dunia, D. Paulin, S. Pournin, and C. Babinet. 1994. Mice lacking vimentin develop and reproduce without an obvious phenotype. *Cell.* 79:679–694.

Dahlstrand, J., V.P. Collins, and U. Lendahl. 1992. Expression of the class VI intermediate filament nestin in human central nervous system tumors. *Cancer Res.* 52:5334–5341.

de Vitry, F., R. Picart, C. Jacques, and A. Tixier-Vidal. 1981. Glial fibrillary acidic protein: a cellular marker of tanycytes in the mouse hypothalamus. *Dev. Neurosci.* 4:457–460.

Eddleston, M., and L. Mucke. 1993. Molecular profile of reactive astrocytes—implications for their role in neurologic disease. *Neuroscience.* 54:15–36.

Franke, W.W., E. Schmid, M. Osborn, and K. Weber. 1979. Intermediate-sized filaments of human endothelial cells. *J. Cell Biol.* 81:570–580.

Frisén, J. 1997. Determinants of axonal regeneration. *Histol. Histopathol.* 12: 857–868.

Frisén, J., C.B. Johansson, C. Török, M. Risling, and U. Lendahl. 1995. Rapid, widespread, and long lasting induction of nestin contributes to the generation of glial scar tissue after CNS injury. *J. Cell Biol.* 131:453–464.

Frisén, J., V.M.K. Verge, S. Cullheim, H. Persson, K. Fried, D.S. Middlemas, T. Hunter, T. Hökfelt, and M. Risling. 1992. Increased levels of trkB mRNA and trkB protein-like immunoreactivity in the injured rat and cat spinal cord. *Proc. Natl. Acad. Sci. USA.* 89:11282–11286.

Fuchs, E., and D.W. Cleveland. 1998. A structural scaffolding of intermediate filaments in health and disease. *Science.* 279:514–519.

Gabbiani, G., E. Schmid, S. Winter, C. Chaponnier, C. de Ckhastony, J. Vandekerckhove, K. Weber, and W.W. Franke. 1981. Vascular smooth muscle cells differ from other smooth muscle cells: predominance of vimentin filaments and a specific alpha-type actin. *Proc. Natl. Acad. Sci. USA.* 78:298–302.

Galou, M., E. Colucci-Guyon, D. Ensergueix, J.-L. Ridet, M. Gimenez y Ribbota, A. Privat, C. Babinet, and P. Dupouey. 1996. Disrupted glial fibrillary acidic protein network in astrocytes from vimentin knockout mice. *J. Cell Biol.* 133:853–863.

Gomi, H., T. Yokoyama, K. Fujimoto, T. Ikeda, A. Katoh, T. Itoh, and S. Itohara. 1995. Mice devoid of the glial fibrillary acidic protein develop normally and are susceptible to scrapie prions. *Neuron.* 14:29–41.

Johansson, C.B., S. Momma, D.L. Clarke, M. Risling, U. Lendahl, and J. Frisén. 1999. Identification of a neural stem cell in the adult mammalian central nervous system. *Cell.* 96:25–34.

Lazarides, E. 1982. Intermediate filaments: a chemically heterogeneous, developmentally regulated class of proteins. *Annu. Rev. Biochem.* 51:219–250.

Lendahl, U., L. Zimmerman, and R. McKay. 1990. CNS stem cells express a new class of intermediate filament protein. *Cell.* 60:585–595.

Li, Z., M. Mericskay, O. Agbulut, G. Butler-Browne, L. Carlsson, L.E. Thornell, C. Babinet, and D. Paulin. 1997. Desmin is essential for the tensile strength and integrity of myofibrils but not for myogenic commitment, differentiation, and fusion of skeletal muscle. *J. Cell Biol.* 6:129–144.

Liedtke, W., W. Edelman, P.L. Bieri, F.C. Chiu, N.J. Cowan, R. Kucherlapati, andp C.S. Raine. 1996. GFAP is necessary for the integrity of CNS white matter architecture and long-term maintenance of myelination. *Neuron.* 17:607–615.

Lin, R.C.S., D.F. Matesic, M. Marvin, R.D. McKay, and O. Brustle. 1995. Re-expression of the intermediate filament nestin in reactive astrocytes. *Neurobiol. Dis.* 2:79–85.

Marvin, M.J., J. Dahlstrand, U. Lendahl, and R.D. McKay. 1998. A rod end deletion in the intermediate filament protein nestin alters its subcellular localization in neuroepithelial cells of transgenic mice. *J. Cell Sci.* 111:1951–1961.

McCall, M.A., R.G. Gregg, R.R. Behringer, M. Brenner, C.L. Delaney, E.J. Galbreth, C.L. Zhang, R.A. Pearce, S.Y. Chiu, and A. Messing. 1996. Targeted deletion in strocyte intermediate filament (GFAP) alters neuronal physiology. *Proc. Natl. Acad. Sci. USA.* 93:6361–6366.

McGowan, K., and P.A. Coulombe. 1998. The wound repair-associated keratins 6, 16 and 17. In Intermediate filaments. *Subcellular Biochemistry.* 31:173–204.

Paladini, R.D., K. Takahashi, N.S. Bravo, and P.A. Coulombe. 1996. Onset of re-epithelialization after skin injury correlates with a reorganization of keratin filaments in wound edge keratinocytes: defining a potential role for keratin 16. *J. Cell Biol.* 132:381–397.

Pekny, M., P. Levéen, M. Pekna, C. Eliasson, C.-H. Berthold, B. Westermark, and C. Betsholtz. 1995. Mice lacking glial fibrillary acidic protein display astrocytes devoid of intermediate filaments but develop and reproduce normally. *EMBO (Eur. Mol. Biol. Organ.) J.* 14:1590–1598.

Pekny, M., K. Stanness, C. Eliasson, C. Betsholtz, and D. Janigro. 1998a. Impaired induction of blood-brain barrier properties in aortic endothelial cells by astrocytes from GFAP-deficient mice. *Glia.* 22:390–400.

Pekny, M., C. Eliasson, C.-L. Chien, L.G. Kindblom, R. Liem, A. Hamberger, and C. Betsholtz. 1998b. GFAP-deficient astrocytes in vitro are capable of stellation when cocultured with neurons and exhibit a reduced amount of intermediate filaments and an increased cell saturation density. *Exp. Cell Res.* 239:332–343.

Pixley, S.K., and J. de Vellis. 1984. Transition between immature radial glia and mature astrocytes studied with a monoclonal antibody to vimentin. *Brain Res.* 317:201–209.

Ridet, J.L., S.K. Malhotra, A. Privat, and F.H. Gage. 1997. Reactive astrocytes: cellular and molecular cues to biological function. *Trends Neurosci.* 20:570–577.

Rutka, J.T., and S.L. Smith. 1993. Transfection of human astrocytoma cells with glial fibrillary acidic protein complementary DNA: analysis of expression, proliferation and tumorigenicity. *Cancer Res.* 53:3624–3631.

Schaeren-Wiemers, N., and A. Gerfin-Moser. 1993. A single protocol to detect transcripts of various types and expression levels in neural tissue and cultured cells: in situ hybridization using digoxigenin-labelled cRNA probes. *Histochemistry.* 100:431–440.

Schnitzer, J., W.W. Franke, and M. Schachner. 1981. Immunocytochemical demonstration of vimentin in astrocytes and ependymal cells of developing and adult mouse nervous system. *J. Cell Biol.* 90:435–447.

Shibuki, K., H. Gomi, L. Chen, S. Bao, J.J. Kim, H. Wakatsuki, T. Fujisaki, K. Fujimoto, A. Katoh, T. Ikeda, et al. 1996. Deficient cerebellar long-term depression, impaired eyeblink conditioning and normal motor coordination in GFAP mutant mice. *Neuron.* 16:587–599.

Tatzelt, J., N. Maeda, M. Pekny, S.-L. Yang, C. Betsholtz, C. Eliasson, A.P. Camerino, S.J. DeArmond, and S.B. Prusiner. 1996. Scrapie in mice deficient for apoliprotein E or glial fibrillary acidic protein. *Neurology.* 47:449–453.

Terzi, F., D. Henrion, E. Colucci-Guyon, P. Federici, C. Babinet, B.I. Levy, P. Briand, and G. Friedlander. 1997. Reduction of renal mass is lethal in mice lacking vimentin. Role of endothelin-nitric oxid imbalance. *J. Clin. Invest.* 100:1520–1528.

Toda, M., M. Miura, H. Asou, S. Toya, and K. Uyemura. 1994. Cell growth suppression of astrocytoma C6 cells by glial fibrillary acidic protein cDNA transfection. *J. Neurochem.* 63:1975–1978.

Tohyama, T., V.M.-Y. Lee, L.B. Rorke, M. Marvin, R.D.G. McKay, and J. Trojanowski. 1992. Nestin expression in embryonic human neuroepithelium and in human neuroepithelial tumor cells. *Lab. Invest.* 66:303–313.

Weinstein, D.E., M.L. Shelanski, and R.K.H. Liem. 1991. Suppression by antisense mRNA demonstrates a requirement for the glial fibrillary acidic protein in the formation of stable astrocytic processes in response to neurons. *J. Cell Biol.* 112:1205–1213.